SYNAPSE 61:500–514 (2007)

Simple Transporter Trafficking Model for Amphetamine-Induced Dopamine Efflux

PRASANNA K. THWAR,[1] BIPASHA GUPTAROY,[2] MINJIA ZHANG,[2] MARGARET E. GNEGY,[2] MARK A. BURNS,[1] AND JENNIFER J. LINDERMAN[1]*
[1]*Department of Chemical Engineering, University of Michigan, Ann Arbor, Michigan 48109*
[2]*Department of Pharmacology, University of Michigan Medical School, Ann Arbor, Michigan 48109*

KEY WORDS enhanced efflux; mathematical model; DA efflux; kinetics

ABSTRACT Amphetamine and its derivatives are important drugs of abuse causing both short-term excitatory and long-term addictive effects. The short-term excitatory effects are linked to amphetamine's ability to maintain high levels of dopamine (DA) outside the cell both by inhibiting DA reuptake after synaptic transmission and by enhancing the efflux of DA from the dopaminergic cells. The molecular mechanisms by which amphetamine elicits the efflux of DA and similar monoamines are still unclear. Recent literature data suggest that trafficking of the monoamine transporters is a phenomenon that underlies observed changes in amphetamine-induced monoamine reuptake and efflux. We develop an ordinary differential equation model incorporating the diverse mechanistic details behind amphetamine-induced DA efflux and demonstrate its utility in describing our experimental data. We also demonstrate an experimental method to track the time-varying concentration of membrane-bound transporter molecules from the DA efflux data. The good fit between our model and the experimental data supports the hypothesis that amphetamine-induced transporter trafficking is necessary to produce extended efflux of DA. This model can explain the relative significance of different processes associated with DA efflux at different times and at different concentration ranges of amphetamine and DA. **Synapse 61:500–514, 2007.**

INTRODUCTION

The localization of dopamine (DA) in limbic and hypothalamic tracts, as well as basal ganglia, integrally involves DA in crucial functions, such as cognition, reward, hormonal regulation, and movement. Consequently, DA plays key roles in the pathology of psychosis, drug abuse, and Parkinson's disease. The regulation of the level of synaptic DA is thus extremely important for normal function. Although exocytotically released DA is inactivated by metabolism, by diffusion and by reuptake, the key regulator of synaptic DA is considered to be reuptake through the Na^+, Cl^--dependent plasmalemmal dopamine transporter (DAT), DAT (Zahniser and Doolen, 2001). DAT is also the site of action of two psychostimulant drugs, amphetamine and cocaine. Both drugs competitively inhibit reuptake of DA, but amphetamine functions as a substrate of DAT while cocaine blocks DAT (Seiden et al., 1993).

The Na^+, Cl^--dependent transporters, including DAT, are considered to function as gated carriers. In that model, the substrate binds to a conformation of the transporter with an open binding site facing the exterior of the cell, followed by a subsequent conformational change that "closes" the exterior site and "opens" an interior site resulting in dissociation of substrate at the opposite side (Rudnick and Clark, 1993; Schenk, 2002). This process is referred to as carrier-mediated diffusion (Stein, 1986). The concept of inward- and outward-facing gates of the Na^+, Cl^--dependent transporters is consistent with the solved crystal structure of a bacterial homologue of Na^+, Cl^--dependent transporters, the $LeuT_{Aa}$ transporter (Yamashita et al., 2005).

Transporter-mediated exchange has been hypothesized to explain the mechanism of action of amphetamine (Fischer and Cho, 1979; Seiden et al., 1993), whereby amphetamine would bind to the exterior face of the transporter and, upon being transported inward along with Na^+ and Cl^-, would increase the concentration of inward-facing transporter as well as the concentration of Na^+ at the inward face of the transporter. A

Contract grant sponsor: Rackham Interdisciplinary Summer Institute, University of Michigan; Contract grant sponsor: Merck Research Laboratories.

*Correspondence to: Jennifer J. Linderman, Department of Chemical Engineering, 2300 Hayward Avenue, 3074 HH Dow, University of Michigan, Ann Arbor, Michigan 48109, USA. E-mail: linderma@umich.edu

Received 15 June 2006; Accepted 3 December 2006

DOI 10.1002/syn.20390

Published online in Wiley InterScience (www.interscience.wiley.com).

consequence of this mechanism would be that one molecule of DA would be released for every molecule of amphetamine taken up. However, results of several studies are inconsistent with this simplistic model and further understanding of the function and regulation of DAT have led to a modification of the hypothesis (Khoshbouei et al., 2004; Sitte et al., 1998) (and see complete discussion in Sulzer et al., 2005). For instance, DAT can also exist in a channel-like mode whereby there is a greater transfer of charge than anticipated by amount of transported substrate (Kahlig et al., 2005; Sonders et al., 1997). Sulzer et al. (2005) have postulated a unified theory of amphetamine-stimulated reverse transport that is a gating mechanism, which combines aspects of facilitated diffusion with its one to one molecule limit with those of a channel.

Another aspect of DAT regulation that can affect influx and efflux characteristics is intracellular trafficking (Gnegy, 2003; Khoshbouei et al., 2004; Zahniser and Doolen, 2001). In heterologous PC12 cells, DAT was shown to internalize at rates of 3–5% per minute (Loder and Melikian, 2003), which greatly exceeds bulk membrane turnover rates (Melikian, 2004). Second messenger signaling has been demonstrated to have profound effects on DAT activity through regulation of surface DAT [for a comprehensive review, see (Zahniser and Doolen, 2001)]. For example, activation of protein kinase C for times greater than 10–15 min significantly reduces DA uptake and, coordinately, reduces cell surface DAT (for a complete review of this well-documented effect, see Zahniser and Doolen, 2001). On the other hand, a short pulse of a protein kinase C-activating phorbol ester increases DA efflux through the DAT (Cowell et al., 2000; Kantor and Gnegy, 1998). Amphetamine itself regulates trafficking of DAT in a biphasic manner. At higher concentrations or longer times, amphetamine treatment of cells results in a reduction of DA uptake and a reduction in surface DAT (Saunders et al., 2000). However, we have demonstrated that, at short times, amphetamine treatment of synaptosomes or heterologous HEK 293 cells results in a significant increase of surface DAT (Johnson et al., 2005). The increase in surface DAT was found at times commensurate with the action of amphetamine in eliciting DA efflux.

The kinetic conditions of amphetamine-stimulated DA efflux have been modeled based on principles of a simple carrier as defined by Stein (1986), using either a 3-state (Jones et al., 1999) or 4-state model (Schenk, 2002). Because AMPH can alter both DAT trafficking and DAT reversal simultaneously, though at different rates and at different levels of intracellular AMPH and DA, a quantitative model is required to understand both the relative contributions of each to the overall AMPH-induced DA efflux, and the temporal dynamics of the process. In this article, we introduce AMPH-induced DAT trafficking as a necessary component to an existing AMPH-induced DAT reversal model for understanding AMPH effects on DA efflux. The model successfully describes AMPH-induced DA efflux in an hDAT-transfected HEK 293 cell system and strongly supports the need to include DAT trafficking in quantitative modeling of DAT efflux.

METHODS

We developed a mathematical model based on transport kinetics to understand the effects of AMPH on DA efflux and DAT trafficking and performed experiments to measure some of the uptake and release parameters of the model. This section explains the model development and the experimental methods used.

Mathematical model

Figure 1 illustrates the processes associated with AMPH-induced DA efflux. Both AMPH and DA are structurally similar and are transported by DAT through similar mechanisms (Fig. 1a, Box 1). DAT molecules on the plasma membrane constantly undergo reorientation between their outward-facing and inward-facing conformations. The ratio of these two conformations regulates the net directional preference of monoamine transport. The competitive transport of AMPH through DAT affects this ratio of DAT conformations and subsequently leads to enhanced DA release. DAT molecules undergo constitutive internalization and may be degraded intracellularly (Daniels and Amara, 1999). Intracellular DAT may also be mobilized back to the surface (Loder and Melikian, 2003). Current theories of AMPH-mediated DA release propose that AMPH plays a significant role in this DAT trafficking (internalization and surface mobilization).

Transport of DA and AMPH by DAT

DAT-mediated transport of monoamine neurotransmitters across the plasma membrane occurs via three sequential steps—binding, DAT reorientation, and release. This transport can be oriented from inside to outside or vice versa. The transported neurotransmitters are slowly metabolized because of the action of enzymatic degradation. Every time an extracellular substrate molecule gets transported to the inside of the cell through DAT, the DAT molecule reorients from an outward-facing configuration to an inward-facing configuration and vice versa. DAT can function bidirectionally to transport substrates from both inside and outside of the cell, though the transport efficiencies for the influx and efflux may differ and depend on the DAT conformation (Chen and Justice Jr, 2000; Khoshbouei et al., 2004; Sitte et al., 1998; Stein, 1986). This bidirectional functionality together with the reversal of the transporter orientation during neurotransmitter transport results in two distinct populations of fully func-

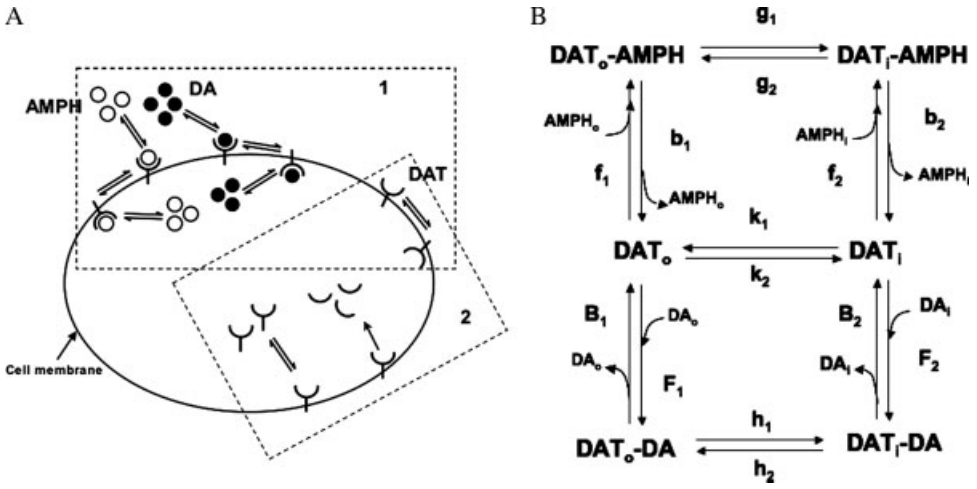

Fig. 1. (**a**) Schematic of the processes by which AMPH affects DA efflux and uptake. Box 1 refers to the membrane-bound processes associated with AMPH-induced DAT reversal. The four states (bound and unbound states of both the inward-facing and outward-facing conformations of DAT) shown represent the current model for explaining the effects of AMPH on DA efflux. Box 2 refers to the processes associated with the trafficking of DAT to and from the membrane, including internalization, surface mobilization, and degradation. DA is represented by filled circles and AMPH by open circles. (**b**) Four-state kinetic scheme for simultaneous transport of DA and AMPH through the membrane-bound DAT. The rate constants for the individual steps are indicated next to the arrows.

tional transporter molecules oriented opposite to each other that can cause influx and efflux of neurotransmitters simultaneously. Thus, conditions that affect the distribution of DAT molecules between these two different populations will also affect the extents and rates of influx and efflux.

The regulated bidirectional transport of DA through DAT in a wild type cell confers the cell with the ability to retain and to cause efflux of DA dependent on the loading conditions (Wilhelm et al., 2006). The structural similarity of AMPH and DA favors a moderately high affinity of AMPH for DAT (Liang and Rutledge, 1982; Wayment et al., 1998; Zaczek et al., 1991). Consequently, AMPH can be transported in a similar fashion through DAT. Under conditions of simultaneous transport of DA and AMPH, the effects of AMPH on individual DAT molecules and on the overall population of DAT molecules become critical. Initially, the effect of AMPH transport through DAT to the cell interior is primarily to reorient the membrane-bound DAT. Later, AMPH is expected to affect the distribution of DAT between the intracellular and membrane-bound domains by mediating the trafficking of DAT molecules. The effect of AMPH on DAT trafficking is highly dependent on the intracellular concentration of AMPH (Kahlig et al., 2006). These phenomena are captured mathematically as described later.

Our semiempirical kinetic model is designed with easily measurable monoamine concentrations as variables and we write ordinary differential equations to describe how these concentrations change with time. Both 3-state (Jones et al., 1999) and 4-state (Schenk, 2002; Wayment et al., 1998) models have been used to describe DAT function; we use the 4-state model, which includes both inward-facing and out-ward facing bound conformations of DAT, for completeness. We write out the individual transport terms in Michaelis–Menton forms by lumping individual rate constants into V_{max} (comparable to the inverse of the resistance term in Stein, 1986) and K parameters (Earles and Schenk, 1999). Also, for understanding the effect of AMPH on DA efflux, we split the efflux term into two to delineate the effects of AMPH from basal efflux.

The rate of change of DA concentration outside the cell, $[DA_o]$, is given by

$$\frac{d[DA_o]}{dt} = \frac{V_1\{[DA_t] - [DA_o]\}}{K_1 + \{[DA_t] - [DA_o]\}} + \frac{V_2[AMPH_o]\{[DA_t] - [DA_o]\}}{K_1 + a[AMPH_o] + \{[DA_t] - [DA_o]\}} - \frac{V_3[DA_o]}{K_3 + [DA_o]} \quad (1)$$

The first term on the right-hand side of the equation where $[DA_t]$ is the total amount of DA inside and outside the cell represents the "basal" efflux of DA in the absence of any other monoamine; the second term refers to the AMPH-mediated DA efflux and is based on the ability of AMPH to induce reversal of DAT conformation and subsequently to cause changes in DA transport; the third term indicates the uptake of DA from outside through the membrane-bound DAT. The "basal" efflux is nonvarying and the AMPH-induced efflux of DA is a function of time. Thus, the total efflux of DA in the presence of AMPH is considered to be a sum of this nonvarying basal efflux and the varying, AMPH-induced efflux. The detailed derivation of the

first two terms is explained in the Appendix (Eq. A11a). It is assumed that all transport of DA across the cell membrane is DAT-mediated and does not occur through processes such as exocytosis or endocytosis. While both DA and AMPH may diffuse in and out of the cell membrane depending on the concentration gradient across the membrane, the extent of diffusional transport in membrane systems expressing DAT is expected to be very low. Sitte et al. (1998) showed that the transport of DA and AMPH across the membrane in DAT-expressing cells is significantly higher than in cells without DAT and is very sensitive to DAT-blocking molecules like cocaine. In our model, we assume a completely nonleaky model for the membrane with all the transport of DA and AMPH regulated by membrane DAT.

In Eq. 1, the extracellular concentration of AMPH can vary with experimental conditions. In such cases, the rate of change of extracellular AMPH concentration, $[AMPH_o]$, can be written as

$$\frac{d[AMPH_o]}{dt} = \frac{V_4[AMPH_i]}{K_4 + [AMPH_i]} + \frac{V_2''[DA_o][AMPH_i]}{K_4 + \alpha''[DA_o] + [AMPH_i]} - \frac{V_5[AMPH_o]}{K_5 + [AMPH_o]}. \quad (2)$$

The first two terms on the right-hand side of Eq. 2 represent the efflux rates of AMPH through DAT while the last term represents the uptake rate of AMPH. It is assumed that since AMPH transport across the membrane, like DA transport, is DAT-mediated, it also follows simple Michaelis–Menton kinetics. The middle term in Eq. 2, representing the effect of DA on AMPH transport, resembles the middle term in Eq. 1. In most experimental measurements of DA efflux, the extracellular concentration of DA is insignificant and hence the middle term can be ignored.

In Eqs. 1 and 2, the V parameters (V_1 through V_5) determine the maximal rates and lump quantities, such as the number of surface transporters and the dominant rate constants in the entire transport process. The K parameters (K_1 through K_4) determine the affinity and the efficiency of binding of the substrate with the different transporter conformations and they lump the rate constants for association and dissociation events. More detail is given in the Appendix. The physical meanings of the parameters are listed in Table I and the full expressions for the lumped parameters can be seen in the Appendix.

DAT trafficking

If one were to assume that basal or constitutive trafficking has no significant effect on the concentration of membrane-bound DAT and that trafficking is unaffected by intracellular AMPH, then the concentration of membrane-bound DAT would remain constant. Consequently, the V parameters that lump the membrane-bound DAT concentration along with other rate constants would also be constant. Quantitative models of AMPH-induced DA efflux to date have included this assumption (Earles and Schenk, 1999; Jones et al., 1999).

However, if DAT trafficking is actively regulated, the concentration of DAT at the membrane will change with time. Thus the maximal transport rates, the V parameters in Eqs. 1 and 2, will become time-dependent and can be expressed as

$$V_1(t) = p_1\ \tilde{n}(t) \quad (3a)$$

$$V_2(t) = p_2\ \tilde{n}(t) \quad (3b)$$

$$V_3(t) = p_3\ \tilde{n}(t) \quad (3c)$$

where $\tilde{n}(t)$ is a dimensionless number representing the time-varying membrane-bound DAT concentration normalized to the initial (before AMPH stimulation) membrane-bound DAT concentration and p's are lumped parameters representing the grouping of rate constants (Eqs. A12 and A13) with the initial membrane-bound DAT concentration. Hence Eq. 1 can be rewritten using Eqs. 3a–3c as

$$\frac{d[DA_o]}{dt} = \frac{p_1\ \tilde{n}(t)\{[DA_t] - [DA_o]\}}{K_1 + \{[DA_t] - [DA_o]\}} + \frac{p_2\ \tilde{n}(t)[AMPH_o]\{[DA_t] - [DA_o]\}}{K_1 + \alpha[AMPH_o] + \{[DA_t] - [DA_o]\}} - \frac{p_3\ \tilde{n}(t)[DA_o]}{K_3 + [DA_o]}. \quad (4)$$

An expression for the time-variant $\tilde{n}(t)$ can be written in terms of the rate of surface mobilization and internalization of the transporter molecules. In the absence of AMPH, we assume that DAT molecules are constitutively internalized and mobilized at a constant rate and hence do not vary much with time. In the presence of AMPH, they are mobilized and internalized at a rate dependent upon the concentration of intracellular AMPH (Kahlig et al., 2006) and given as

$$\frac{d\tilde{n}(t)}{dt} = \frac{\tilde{V}_6[AMPH_i]}{K_6 + [AMPH_i]} - \frac{\tilde{V}_7[AMPH_i]}{K_7 + [AMPH_i]} \quad (5)$$

where the terms with ($\sim$) are obtained by normalizing the respective rates to the initial (before AMPH stimulation) membrane-bound DAT concentration. Table I gives the definitions and physical meanings of the parameters in Eq. 5.

Solution method

Equations 2, 4, and 5 can be solved simultaneously using Mathematica (Wolfram Research Inc., Champaign, IL) to obtain the time-varying extracellular DA concen-

TABLE I. List of parameters used in the model for AMPH-induced DA release

Parameters	Expression	Physical meaning	Units	Values used in the model
p_1	Equation (A.13) in Appendix	Lumped parameter of rate constants associated with basal efflux of DA along with the initial concentration of total membrane-bound DAT	pmol/mg/s	11.5
p_2	Equation (A.14) in Appendix	Lumped parameter of rate constants associated with AMPH-induced DA efflux only, along with the initial concentration of total membrane-bound DAT	s^{-1}	0.028
p_3		Rate constants associated with DA uptake lumped with the initial concentration of total membrane-bound DAT	pmol/mg/s	11.5
V_4		Maximal uptake rate of AMPH through DAT	pmol/mg/s	1
$\tilde{V}_6$		Maximal rate of AMPH-induced surface mobilization of DAT, normalized to the initial membrane-bound DAT concentration before AMPH stimulation	s^{-1}	1
$\tilde{V}_7$		Maximal AMPH-induced DAT internalization rate, normalized to the initial membrane-bound DAT concentration before AMPH stimulation	s^{-1}	2.46 ± 0.022 (1 μM AMPH), 2.31 ± 0.040 (3 μM AMPH), 2.28 ± 0.033 (10 μM AMPH)
K_1	Equation (A.15) in Appendix	Measure of affinity of DA to the inward-facing conformation of DAT	pmol/mg	3500
K_3		Measure of affinity of DA to the outward-facing conformation of DAT	pmol/mg	410
K_4		Measure of affinity of AMPH to the outward-facing conformation of DAT	pmol/mg	50
K_6		Measure of affinity of intracellular AMPH towards the molecular machinery that mobilizes DAT to the membrane from the cytosol	pmol/mg	28.33 ± 1.67
K_7		Measure of affinity of intracellular AMPH towards the intracellular molecular machinery involved in the internalization of DAT from the membrane	pmol/mg	73.33 ± 1.67
a	Equation (A.16) in Appendix	Lumped parameter signifying the relative dominance of extracellular concentration of AMPH in DA release	Dimensionless	2.5
β	$\frac{V_5}{K_5}$	Time constant signifying the effectiveness of AMPH release process	s^{-1}	0.1

tration for a particular set of initial conditions. Appropriate choice of experimental conditions can simplify the solution. The initial conditions for the concentration variables are typically one of four sets (zero-cis, zero-trans, infinite-cis, or infinite-trans; cis is the intracellular side and trans is the extracellular side). For the experiments described in this article, the initial conditions for AMPH-induced DA efflux are zero-trans for DA (i.e., $[DA_o]_{t=0} = 0$ and $\{[DA_t]-[DA_o]\}_{t=0}$ = DA loading in the cell), and zero-cis for AMPH (i.e., $[AMPH_i]_{t=0} = 0$ and $[AMPH_o]_{t=0}$ = AMPH concentration used to stimulate DA efflux).

Experimental methods

Data for model fitting and analysis were obtained by monitoring the time-dependent AMPH-induced DA efflux in a continuous perfusion protocol. We also conducted steady state DA efflux experiments in petri dishes to explore some steady state characteristics of the system.

Measurement of AMPH-induced DA efflux

Confluent HEK 293 cells stably transfected with hDAT (hDAT-HEK described in Hastrup et al., 2001; Khoshbouei et al., 2004) were cultured in 100-mm plates and then incubated with 15 μM unlabeled DA for 30 min at 37°C. DA taken up during this incubation (loaded DA amount) was measured by homogenizing and lysing the suspended cells and measuring the DA content in the supernatant by high-performance liquid chromatography (HPLC) with electrochemical detection (HPLC-EC). The total DA accumulated in the cells over the 15-min period was 3000 pmol of DA/mg total protein. The total protein content of the cells was measured by Bio-Rad DC Protein Assay (Bio-Rad Laboratories, Hercules, CA). Following incubation, cells were washed twice with a Krebs-Ringer-Hepes (KRH) buffer (25 mM Hepes, pH 7.4, 125 mM NaCl, 4.8 mM KCl, 1.2 mM KH_2PO_4, 1.3 mM $CaCl_2$, 1.2 mM $MgSO_4$, 5.6 mM glucose, and 1 mM tropolone) and resuspended in 900 μl of the same. The cell suspension (800 μl) was equally split and loaded onto four different chambers in the Brandel superfusion apparatus (Brandel SF-12, Gaithersburg, MD) and the remaining 100 μl of the cells were used to measure protein. The cells were washed with KRH buffer for 30 min before perfusion with either 0, 1, 3, or 10 μM AMPH for a full 50 min. The flow rate was 100 μl/min. DA released from cells in response to AMPH stimulation was collected in 5-min intervals and analyzed using HPLC-EC. The amount of DA collected at each 5-min interval was then normalized to the total amount of DA loaded. To compare the amount of DA collected from different perfusion chambers, the amount of DA collected (expressed in pmol released/pmol loaded) was then multiplied by the average loading concentration of DA (3000 pmol DA/mg

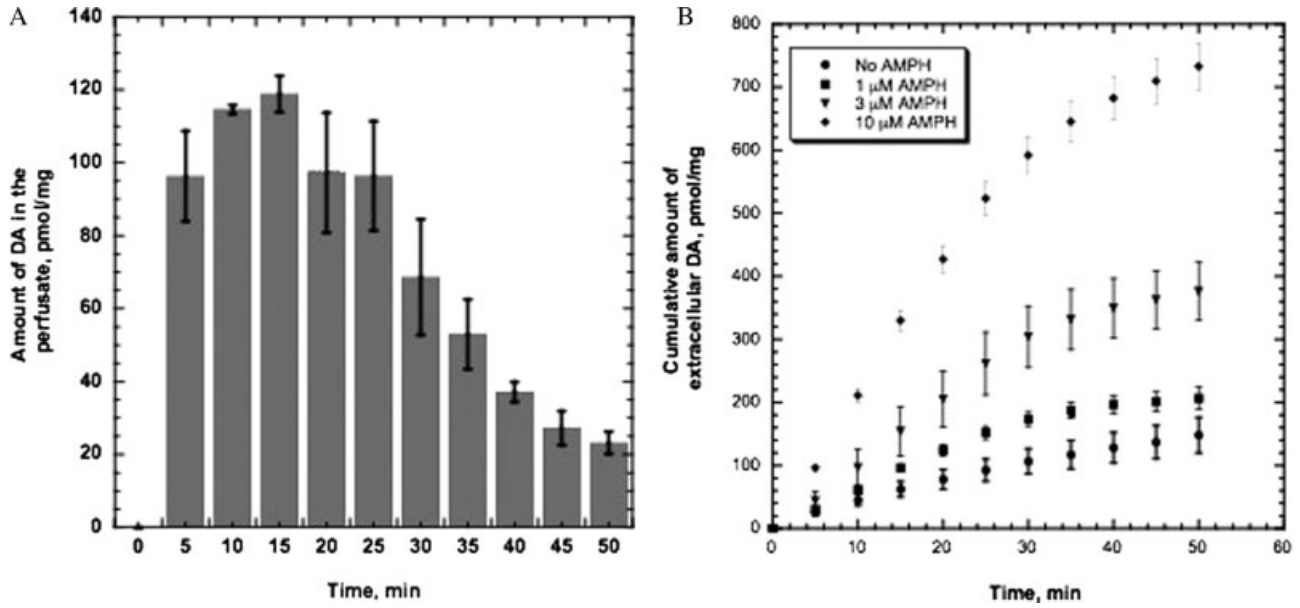

Fig. 2. AMPH-induced DA efflux. (**A**) The amount of DA in the extracellular perfusate, released from hDAT-HEK cells perfused with 10 μM AMPH and measured at 5-min collection intervals, using HPLC-EC. (**B**) Cumulative time-varying DA release for four perfusion concentrations of AMPH (0, 1, 3, and 10 μM). The data points are mean concentrations calculated from three cell populations and the error bars represent the standard error of the mean.

total protein) to give amount of DA released in each chamber in units of pmol of DA/mg total protein. The variability between the chambers comes from the difference in the number of cells loaded in them. Further, for comparison with the model, the amounts of DA released in each of the successive 5-min intervals (Fig. 2a) were added to give a cumulative amount of DA released over a specific period of time (Fig. 2b).

Measurement of basal efflux of DA for different loading concentrations

Confluent hDAT-HEK 293 cells were transferred from flasks to 35-mm petri dishes and incubated with 2 ml of media containing 30 nM of [^{3}H]DA (Perkin Elmer, Boston, MA, specific activity 59.7 μCi/nmol) with varying concentrations of unlabeled DA (0.5, 1, 5 μM). Following incubation for 10 min at 37°C, the media was removed and the cells were washed twice with KRH buffer. One milliliter of KRH buffer was added to the culture dish. After 10 min, 200-μl aliquots of the media were placed into ScintiVerse BD and the extracellular [^{3}H]DA was determined in a Beckman LS 5800 scintillation counter.

RESULTS

Model analysis

Simple analyses of Eqs. 2, 4, and 5 can provide both valuable insights into the behavior of the system under particular circumstances and initial estimates for some model parameters.

Basal DA efflux (no AMPH)

In the absence of AMPH (and hence $\tilde{n} = 1$), the rate of change of extracellular DA concentration (Eq. 4) can be written as

$$\frac{d[DA_o]}{dt} = \frac{p_1\{[DA_t] - [DA_o]\}}{K_1 + \{[DA_t] - [DA_o]\}} - \frac{p_3[DA_o]}{K_3 + [DA_o]}. \quad (6)$$

Many DA efflux experiments are performed in zero-trans conditions and so the initial concentration of extracellular DA is zero (i.e., $[DA_o]_{t=0} = 0$). Under these conditions, the DA efflux rate, measured as the rate of change of extracellular DA concentration, is a maximum initially and gradually falls off as the intracellular DA levels are depleted. In the absence of reuptake, complete emptying of the intracellular DA could be expected. But there is also transport of DA back into the cell through the same transporters. Consequently, the DA efflux rate falls significantly even after a moderate amount of efflux. As detailed later, these temporal dynamics simplify further for particular cases.

Moderate to low DA-transporter binding affinity [large K value(s)]. We consider three cases. First, if the K values on either side of the cell membrane are significantly larger than the relevant DA concentrations (i.e., $K_1 \gg \{[DA_t]–[DA_o]\}$) and $K_3 \gg [DA_o]$), Eq. 6 can be simplified to

$$[DA_o] = \frac{A}{B}\left(1 - e^{-Bt}\right) \quad (7)$$

where

$$A = \frac{p_1}{K_1}[DA_t] \text{ and } B = \frac{p_1}{K_1} + \frac{p_3}{K_3}.$$

Such substrates (with large K values) typically are required to be present at a high concentration to achieve substantial efflux or uptake rates. They are likely to need more association–dissociation events per transport of substrate molecule (see Appendix for relationship of K values to rate constants). In such cases, if the transport efficiency defined by p_i/K_i does not change on either side of the membrane during the course of basal efflux of substrates, then the steady state concentration of extracellular DA, $[DA_o]_{t=\infty}$, is purely a function of the DA concentration loaded inside the cell initially given as

$$[DA_o]_\infty = \frac{A}{B} = \left(\frac{\frac{p_1}{K_1}}{\frac{p_1}{K_1} + \frac{p_3}{K_3}}\right)[DA_t]. \quad (8)$$

Thus if the steady state concentration of extracellular DA does not vary linearly with the loading concentration, it suggests either that K parameter values are not significantly larger than the loading DA concentration or that the transport efficiencies on either of the sides vary during the transport. The transport efficiency could change either because of a change in the number of transporters with a favorable conformation for transport on the membrane or because of a change in the binding efficiency of the substrates with the respective transporters.

Second, if the binding affinity of DA for the inward-facing DAT is very high (i.e., $K_1 \ll \{[DA_t]–[DA_o]\}$) and that for the outward-facing DAT is low (i.e., $K_3 \gg [DA_o]$), then the time-dependent concentration of extracellular DA is given by

$$[DA_o] = \frac{p_1}{\left(\frac{p_3}{K_3}\right)}\left(1 - e^{-\left(\frac{p_3}{K_3}\right)t}\right) \quad (9)$$

and the steady state concentration of extracellular DA would then be a constant and independent of the loaded DA concentration as given by

$$[DA_o]_\infty = \frac{p_1 K_1}{p_3}. \quad (10)$$

Third, if the binding affinity of DA for the outward-facing DAT is high (i.e., $K_3 \ll [DA_o]$) and that for the inward-facing DAT is low (i.e., $K_1 \gg \{[DA_t]–[DA_o]\}$), then the time dependent concentration of $[DA_o]$ is given by

$$[DA_o] = \left(\left(\frac{p_1[DA_t]}{K_1}\right) - p_3\right)t. \quad (11)$$

According to Eq. 11, the concentration of extracellular DA is either monotonically increasing or decreasing with time depending upon the values of the parameters involved.

High DA-transporter binding affinity (small K values). If both the K parameter values are significantly smaller than the respective DA concentrations, then the extracellular DA concentration is a simple monotonic function of time as given by

$$[DA_o] = (p_1 - p_3)t. \quad (12)$$

In such cases, the limiting phenomena in the transport of DA from outside to inside or vice versa is not the binding affinity but the maximal transport rates constituted by the total number of carriers and their rates of switching conformations.

Equations 8–12 thus suggest useful tests to assess the relative magnitude of K on either side of the cell membrane.

AMPH-induced DA efflux

The middle term in Eq. 4 represents the efflux of DA because of AMPH. If $K_1 \gg a\ [AMPH_o] + \{[DA_t]–[DA_o]\}$ and if $[AMPH_o]$ remains constant (constant perfusion) or decreases with time due to uptake (pulse stimulation), then the rate of enhanced DA efflux following AMPH stimulation should be monotonically decreasing, assuming $\tilde{n}$ is a constant throughout the efflux process. But if $\tilde{n}$ changes due to a change in the transporter concentration on the cell membrane, then the enhanced efflux rate may exhibit different kinetics.

The rate of change of $\tilde{n}$ is quantitatively described by Eq. 5. An analysis similar to that earlier provides useful insights for the K value. If both the K values in Eq. 5 are much smaller than $[AMPH_i]$, then $\tilde{n}$ is either linearly increasing or decreasing with time. If both K values are much larger than $[AMPH_i]$ and if $[AMPH_i]$ increases with time due to uptake, then also $\tilde{n}$ is either monotonically increasing or decreasing. As a third possibility, if the relative magnitudes of the K values with respect to $[AMPH_i]$ changes with time (i.e., at short time periods following AMPH stimulation, $K_6, K_7 \gg [AMPH_i]$ and later, $K_6, K_7 \ll [AMPH_i]$), then $\tilde{n}$ may exhibit a maximum or a minimum. Following this, when $\tilde{n}$ exhibits a maximum, $\tilde{V}_6/K_6 > \tilde{V}_7/K_7$ at short time intervals and $\tilde{V}_7 > \tilde{V}_6$ at longer time periods and the signs reverse for the respective time intervals when $\tilde{n}$ exhibits a minimum. This information is useful in estimating values for V_6, V_7, K_6, and K_7.

Model testing

In this section, we demonstrate the applicability of the model developed and analyzed earlier to DA release experiments performed with or without external AMPH stimulation. These experiments are designed to facilitate estimation of the model parameters either directly or indirectly. Later, we also illustrate the AMPH-induced DAT trafficking effects by interpreting the experimental results using our model.

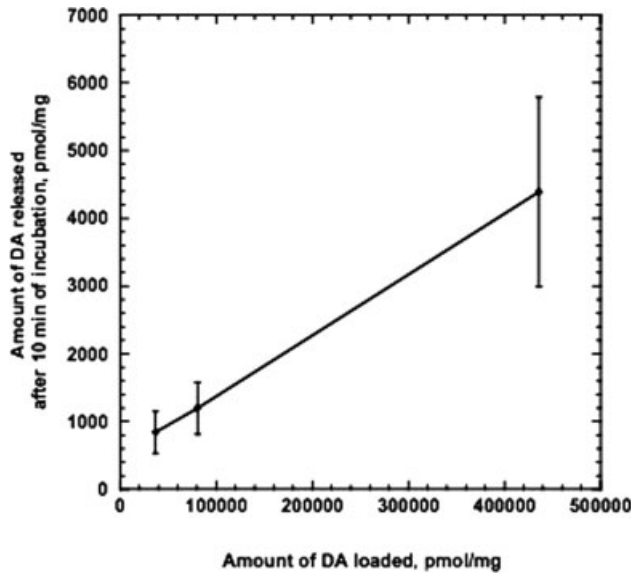

Fig. 3. The steady state concentration of released DA after basal DA efflux follows a linear relation when plotted against the loaded concentration with a regression coefficient $R^2 = 0.9999$ and a P-value of 0.006 for the independent variable. The cells were loaded with either 0.5, 1, or 5 μM [^{3}H]DA for 10 min at 37°C. After loading, the cells were washed twice and then transferred to KRH buffer solution. The radioactivity due to released DA in the buffer solution was then measured after 10 min, a point at which steady state would be reached.

DA efflux rate rises and then falls in response to continuous long-term AMPH stimulation

The amount of DA in the perfusate at 5 min intervals in response to perfusion by 10 μM AMPH concentration is shown in Figure 2a. It can be seen that the amount of DA released in a 5-min interval increases and reaches a maximum and subsequently falls with time. Similar trends were observed for other nonzero concentrations of AMPH (data not shown). For comparison with the model, these data were then converted into cumulative extracellular DA amounts varying with time following AMPH stimulation (Fig. 2b). This implies that AMPH entry into the cell induces a time-dependent phenomenon that directly affects the DA efflux profile. The rate of change of extracellular DA concentration eventually goes to zero. This may imply either equal magnitudes of uptake and efflux rates or the total shut-off of both processes, possibly due to the absence of membrane-bound transporters.

Basal efflux parameters computed from efflux in the absence of AMPH stimulation

Under zero-trans conditions, basal DA efflux (no AMPH) also saturates with time (bottom curve in Fig. 2b). This is consistent with a moderate to low DA-transporter binding affinity, i.e., large K_1 and/or K_3 values, via Eqs. 8 or 9. We then measured the steady state basal efflux of DA under different DA loading concentrations, as shown in Figure 3. The final released DA concentration is a linear function of the loaded DA concentration. According to the analysis presented earlier, this suggests that $K_1 \gg [DA_i]$ and $K_3 \gg [DA_o]$, and that the steady state concentration of extracellular DA is described by Eq. 8.

Utilizing the restrictions on K_1 and K_3 determined earlier, numerical values for the parameters associated with basal DA efflux were computed from the transient efflux data collected in the absence of AMPH stimulation. The parameters p_1, p_3, K_1, and K_3 were determined by fitting Eq. 6 to the basal efflux data (Fig. 2b, no AMPH). Since p_1 and p_3 represent lumped rate constants determining the maximal transport rates of DA to the inside and outside of the cell in the absence of AMPH, we assumed that they are equal in magnitude. However the affinities of DA to the outward-facing and inward-facing DAT were allowed to be different, thus resulting in different overall efficiencies of DA uptake and efflux even in the absence of AMPH. The values computed for p_1, p_3, K_1, and K_3 are shown in Table I.

Quantification of DAT trafficking

In our model, the parameter $\tilde{n}(t)$ quantifies DAT trafficking (see Eq. 5). Combined with the model, the experimental data can give a measure of DAT trafficking upon AMPH stimulation. The time-varying profile of $\tilde{n}(t)$ was extracted from our experimental data of time-varying extracellular concentration of DA (Fig. 2b) using

$$\tilde{n}(t) = \frac{\dfrac{d[DA_o]}{dt}}{\dfrac{p_1\{[DA_i]-[DA_o]\}}{K_1+\{[DA_i]-[DA_o]\}} + \dfrac{p_2[AMPH_o]\{[DA_i]-[DA_o]\}}{K_1+a[AMPH_o]+\{[DA_i]-[DA_o]\}} - \dfrac{p_3[DA_o]}{K_3+[DA_o]}} \tag{13}$$

The results of this computation are shown in Figure 4. Note that $\tilde{n}(t)$ exhibits a maximum around 15–25 min following AMPH stimulation and that there is a 40% increase in surface expression of DAT at the highest concentration of AMPH tested (10 μM). This corresponds to rapid surface mobilization of DAT initially and then a rather slow internalization of DAT at longer time periods following AMPH stimulation. Our findings are consistent with the DAT trafficking observed through direct visualization and measurement of surface DAT (Johnson et al., 2005). In addition, from the analysis described earlier, a maximum in the profile of

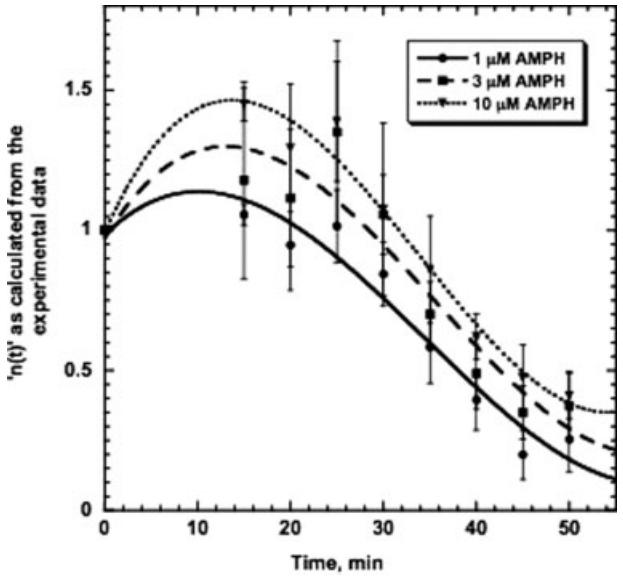

Fig. 4. The time-varying profile of $\tilde{n}(t)$, the membrane-bound DAT concentration normalized to the initial (before AMPH stimulation) membrane-bound DAT concentration, as extracted from the experimental data of Figure 2b, using Eq. 13 for all nonzero values of time. At $t = 0$, $\tilde{n}(t)$ was set at a value of 1. The data points represent the mean values ($n = 3$) and the lines are cubic polynomial fits of the data.

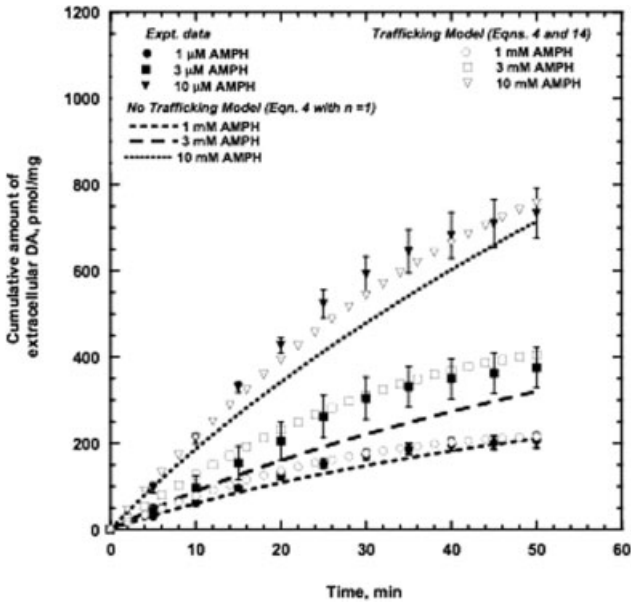

Fig. 5. AMPH-induced DA release data with model fits. Experimental data (filled symbols with standard error of the mean as a vertical error bar) were fitted to both the mathematical models—without trafficking (dotted lines) and with trafficking (open symbols). The trafficking model fits the data better than the model without trafficking effects. For no trafficking model, Eq. 4 was used with constant value of $\tilde{n} = 1$. For trafficking model, Eq. 14 was solved simultaneously with Eq. 4 with an initial value of $\tilde{n} = 1$.

$\tilde{n}(t)$ restricts the parameters to the range where $\tilde{V}_6/K_6 > \tilde{V}_7/K_7$ and $\tilde{V}_7 > \tilde{V}_6$. These guidelines were used later in fitting the model to the experimental data.

Trafficking model fits AMPH-induced DA efflux data better than existing model

The ability of the trafficking model (our model) and that without trafficking (existing model) for AMPH-induced DA efflux to fit the data of Figure 2b was tested. In our continuous cell perfusion protocol, because the extracellular concentration of AMPH was maintained at a constant value (0, 1, 3, or 10 μM), Eq. 2 can be eliminated. In addition, Eq. A20 can be used to approximate the intracellular AMPH concentration. Using Eq. A20, Eq. 5 becomes

$$\frac{d\tilde{n}(t)}{dt} = \frac{\tilde{V}_6\left\{\dfrac{V_4[AMPH^*_o]}{K_4 + [AMPH^*_o]}\dfrac{1}{\beta}\left(1 - e^{-\beta t}\right)\right\}}{K_6 + \left\{\dfrac{V_4[AMPH^*_o]}{K_4 + [AMPH^*_o]}\dfrac{1}{\beta}\left(1 - e^{-\beta t}\right)\right\}} - \frac{\tilde{V}_7\left\{\dfrac{V_4[AMPH^*_o]}{K_4 + [AMPH^*_o]}\dfrac{1}{\beta}\left(1 - e^{-\beta t}\right)\right\}}{K_7 + \left\{\dfrac{V_4[AMPH^*_o]}{K_4 + [AMPH^*_o]}\dfrac{1}{\beta}\left(1 - e^{-\beta t}\right)\right\}} \quad (4)$$

where $[AMPH^*_o]$ is the value of the constant extracellular AMPH concentration maintained throughout the experiment and β is a time constant defined in the Appendix.

The experimental data on AMPH-induced DA efflux were fitted to Eqs. 4 and 14 (Fig. 5). To do this, we held the parameters describing basal efflux data at the values deduced earlier, and we constrained parameters $\tilde{V}_6$, $\tilde{V}_7$, K_6, and K_7 as described earlier. The parameters were fitted to individual data sets ($n = 3$) and then averaged to give the final values used for generating the model predictions in Figure 5. Table I lists the values of all 13 model parameters.

For comparison, the data of Figure 5 were also fit to a model that does not include trafficking of transporters. Equation 4 reflects the model without trafficking when the parameter $\tilde{n}(t)$ is treated as constant with a value of unity. Since the basal efflux parameters should be the same for this case, the same set of values of p_1, K_1, p_3, and K_3 were used.

As seen in Figure 5, the concentration of extracellular DA increases almost linearly with time initially and then begins to plateau at a value dependent on the extracellular (constant) AMPH concentration. The trafficking-based model shows excellent agreement with the experimental data, while the model without trafficking of transporters consistently underpredicts the extracellular DA concentration, indicating that the assumption of constant membrane-bound DAT concentration is inadequate to explain efflux at longer time periods.

DISCUSSION

In this article, we test whether AMPH-induced DAT reversal is sufficient to explain the enhanced DA efflux following AMPH stimulation in hDAT-HEK cells through quantitative modeling and analysis of DA

efflux data. The excellent agreement between our model and the experimental data on DA efflux in response to continuous AMPH stimulation strongly suggests the need to include the effects of AMPH on DAT trafficking in assessing the effects of AMPH on DA efflux. We report that the current quantitative model for DA efflux, without the trafficking effects, consistently underpredicts the extracellular DA concentration resulting from the efflux. Even a trafficking model considering only the AMPH-induced internalization of DAT, without considering the initial AMPH-induced increase in surface DAT, would not be sufficient to explain the experimentally observed trends of $\tilde{n}(t)$. We further qualitatively substantiate the experimental observation of Johnson et al., (2005); in our model the surface expression of DAT undergoes a short-term increase before it falls due to internalization.

Most investigations of the effects of AMPH on DA efflux in isolated cell systems or synaptosomal preparations measure short term or transient stimulation by AMPH (Kahlig et al., 2005; Kantor et al., 2002; Khoshbouei et al., 2004). To our knowledge, our data are the first measuring DA efflux during a persistent stimulation by AMPH on isolated cells. A longer stimulation by AMPH is physiologically relevant since the half-life of AMPH in the rat is 70 min and is 12 h in the human (Cho et al., 2001). Since some of the effects of AMPH surface only after a longer incubation time (>10 min), persistent stimulation for the entire duration of the experiment enables us to see the gradual unfolding of the dynamic events. In addition, the persistent stimulation by AMPH creates a higher intracellular concentration of AMPH, making AMPH-induced DAT trafficking more pronounced. In vivo, a subcutaneous injection of AMPH in the rat results in elevated levels of tissue AMPH for at least 60 min, although levels peak at 30 min (Kuczenski et al., 1997).

The fitting of our experimental data to the model supports to some extent the facilitated exchange hypothesis that inward transport of AMPH promotes an inward-facing conformation of DAT leading to enhanced outward transport of DA. The relative measures of the different parameters provide very useful qualitative explanations. The affinity of DA for the outward-facing DAT is about 8.5 times stronger than for the inward-facing DAT as noted from the values of K_1 and K_3($K_1/K_3 = 3500/410 = 8.53$). The ratio ($V/K$) provides a measure of efficiency of the carrier-mediated transport. From the values listed in Table I, it can be inferred that the efficiency of uptake process ($V_3/K_3 = 0.028$) is roughly 10 times greater than the basal efflux of DA ($V_1/K_1 = 0.003$). Both theoretical and experimental studies confirm such an asymmetry of transport through the same transporter molecule (Chen and Justice Jr, 2000; Khoshbouei et al., 2004; Sitte et al., 1998; Stein, 1986). Since DAT is primarily designed for uptake of DA after synaptic transmission, these values are in good agreement with the current understanding of DAT function. From the fitted value for β, the efficiency of AMPH efflux ($V_5/K_5 = 0.1$) is about 30 times greater than that of DA. Hence, it can be easily inferred that under basal conditions, DA has less tendency than AMPH to be released through DAT. If reversal of DAT conformation were to be the only effect of AMPH on DAT-mediated DA transport (facilitated exchange theory), then the efflux of DA would not be substantial as DA is still not the preferred substrate for efflux in the presence of AMPH. Also, in purely transporter-mediated exchange, the DA efflux would happen concurrently with the uptake of AMPH. Since the initial intracellular and extracellular concentrations of AMPH are zero and maximum, respectively, in our experiments, the transporter-mediated AMPH uptake rate is expected to be maximal at the beginning. Our recent experiments of AMPH uptake (unpublished results) also confirm this. However, our experimental data (Fig. 2a) indicate that the DA efflux goes through a maximum 15–25 min after AMPH stimulation. This suggests that facilitated exchange alone cannot explain the temporal efflux profile of DA following AMPH stimulation. We explain this inadequacy by suggesting that AMPH affects DA transport by mediating time-dependent changes in DAT expression on the membrane.

Our transporter trafficking model captures the data seen in Figure 4. According to our model, upon entering the cell, AMPH interferes with the constitutive DAT trafficking process by catalyzing increased surface expression initially and then internalization. Specifically, we find that the normalized concentration of DAT, $\tilde{n}(t)$, changes with time after AMPH stimulation, going through a maximum around 15–25 min before declining below the initial value after approximately an hour. Recent data obtained in the Gnegy laboratory demonstrated an increase in surface DAT in hDAT-HEK cells very shortly after addition of AMPH (Johnson et al., 2005). This AMPH-mediated increase in surface DAT was detected both by biotinylation and [^{3}H]WIN35428 binding. The increases in surface DAT were on the order of 50–80%, which are comparable to the 40% increase in our experimentally-derived $\tilde{n}(t)$ (Fig. 4). In our experiments, since the outside AMPH concentration is held constant, the intracellular AMPH concentration is also expected to reach a constant value after some time. In fact, the value of β obtained by model fitting indicates that the intracellular AMPH concentration reaches 95% of the steady state value in 15 min. We predict from the observation of the fitted values of $\tilde{V}_6$, K_6, $\tilde{V}_7$, and K_7 that AMPH-induced surface mobilization of DAT starts immediately after a lower threshold of intracellular AMPH concentration is reached and the regulated internalization operates after a slightly higher threshold of intracellular AMPH concentration is reached. These predictions have been verified in hDAT-HEK cells in the literature, using techniques of biotinylation and confocal microscopy. Johnson et al. (2005) reported rapid (30 s^{-1} min) increases in surface DAT in rDAT-GFP-HEK cells following incubation with 3 μM AMPH. Incubations with

2 μM AMPH for 1 hr (Saunders et al., 2000) or 10 μM AMPH for >10 min (Kahlig et al., 2004) resulted in a robust internalization of hDAT from the surface of hDAT-HEK cells. The use of advanced microscopic visualization tools (confocal fluorescence microscopy, total internal reflection microscopy) and single cell experimental techniques to capture the trafficking of DAT molecules and molecular transport in real time (Mason et al., 2005; Troyer and Wightman, 2002) will undoubtedly give the best estimates of the constants in our model.

The mechanism by which AMPH causes the active redistribution of DAT is not known but may involve second messengers, particularly protein kinases (Park et al., 2003; Pristupa et al., 1998). Protein kinase C and intracellular Ca^{2+} were found to be essential for AMPH action (Gnegy et al., 2004; Kantor et al., 2001) and may affect the trafficking of DAT as well as the ability of AMPH to elicit efflux of DA. Protein kinase C is known to have profound effects on internalization of DAT (see reviews, Zahniser and Doolen, 2001; Zhang et al., 1997). Conventional Ca^{2+}-dependent protein kinase C isotypes were found to be important for the down regulation of hDAT expressed in Xenopus oocytes (Doolen and Zahniser, 2002). Different isotypes of protein kinase C could mediate both exocytotic and endocytotic trafficking of DAT. Na^+,K^+-ATPase is another transporter whose trafficking is regulated biphasically by PKC through direct phosphorylation of the transporter at different sites by different PKC isozymes (Budu et al., 2002; Efendiev et al., 1999).

Since the main focus of our modeling approach is to construct a simple model that explains long term AMPH-induced DA efflux data in nondopaminergic cells, it cannot be claimed exhaustive. Some possible effects of AMPH are ignored either as a compromise for simplicity of the model or as a consideration of their relative insignificance. For example, AMPH, being lipophilic, can also diffuse through the plasma membrane and produce changes in the intracellular and extracellular DA concentration (Mack and Bonisch, 1979; Romanenko et al., 1998). But such passive transport causes only an increase in the intracellular concentration of AMPH and does not contribute to the reversal of DAT because there would be no build-up of intracellular Na^+ at the inner face of the transporter (Khoshbouei et al., 2003; Pifl and Singer, 1999). AMPH has been shown to cause changes in intracellular pH (Sulzer et al., 1993). However, it is still unresolved if the pH change specifically affects DAT-mediated monoamine transport and so we did not include that in our model. In dopaminergic cells, where intracellular DA concentration is tightly regulated by VMAT2 expressed on the vesicular membrane, we would need to account for the AMPH effects on VMAT2-mediated DA transport from the vesicles. Since our HEK system does not express VMAT2, it is not included in our model. The ability of AMPH to block VMAT2 controls the maximal amount of DA that will be released in response to AMPH, but DAT, not VMAT2, is essential for AMPH's ability to elicit outward transport of DAT (Fon et al., 1997; Jones et al., 1998; Pifl et al., 1995). Because a rapid AMPH-mediated increase in DAT was found in synaptosomes as well as HEK cells (Johnson et al., 2005), we anticipate that our model will be applicable in physiological systems.

Though our model is semiempirical, it captures the major features of AMPH-induced DA efflux. Since the model is constructed from a Michaelis–Menton approach, the parameters in the model are not specific to any experimental technique. This provides the model with a wide range of applicability and testability, including informing the design of particular experiments to test different hypotheses. The experimental design in this article requires only the measurement of extracellular concentration of DA over time. Combined with the knowledge of few initial conditions, our model provides a simple and an effective way to test the role of DAT trafficking in DA release.

REFERENCES

Britton HG. 1977. Calculation of steady-state rate equations and the fluxes between substrates and products in enzyme reactions. Biochem J 161:517–526.

Budu CE, Efendiev R, Cinelli AM, Bertorello AM, Pedemonte CH. 2002. Hormonal-dependent recruitment of Na^+, K^+-ATPase to the plasmalemma is mediated by PKC β and modulated by $[Na^+]i$. Br J Pharmacol 137:1380–1386.

Chen N and Justice Jr JB. 2000. Differential effect of structural modification of human dopamine transporter on the inward and outward transport of dopamine. Mol Brain Res 75:208–215.

Cho AK, Melega WP, Kuzenski R, Segal DS. 2001. Relevance of pharmacokinetic parameters in animal models of methamphetamine abuse. Synapse 39:161–166.

Cowell RM, Kantor L, Hewlett GH, Frey KA, Gnegy ME. 2000. Dopamine transporter antagonists block phorbol ester-induced dopamine release and dopamine transporter phosphorylation in striatal synaptosomes. Eur J Pharmacol 389:59–65.

Daniels GM, Amara SG. 1999. Regulated trafficking of the human dopamine transporter. Clathrin-mediated internalization and lysosomal degradation in response to phorbol esters. J Biol Chem 274: 35794–35801.

Doolen S, Zahniser NR. 2002. Conventional protein kinase C isoforms regulate human dopamine transporter activity in Xenopus oocytes. FEBS Lett 516:187–190.

Earles C, Schenk JO. 1999. Multisubstrate mechanism for the inward transport of dopamine by the human dopamine transporter expressed in HEK cells and its inhibition by cocaine. Synapse 33:239–238.

Efendiev R, Bertorello AM, Pedemonte CH. 1999. PKC-β and PKC-ζ mediate opposing effects on proximal tubule Na^+, K^+-ATPase activity. FEBS Lett 456:45–48.

Fischer JB, Cho AK. 1979. Chemical release of dopamine from striatal homogenates: Evidence for an exchange diffusion model. J Pharmacol Exp Ther 208:203–209.

Fon EA, Pothos EN, Sun BC, Killeen N, Sulzer D, Edwards RH. 1997. Vesicular transport regulates monoamine storage and release but is not essential for amphetamine action. Neuron 19:1271–1283.

Gnegy ME. 2003. The effect of phosphorylation on amphetamine-mediated outward transport. Eur J Pharmacol 479:83–91.

Gnegy ME, Khoshbouei H, Berg KA, Javitch JA, Clarke WP, Zhang M, Galli A. 2004. Intracellular Ca^{2+} regulates amphetamine-induced dopamine efflux and currents mediated by the human dopamine transporter. Mol Pharmacol 66:137–143.

Hastrup H, Karlin A, Javitch JA. 2001. Symmetrical dimer of the human dopamine transporter revealed by cross-linking Cys-306 at the extracellular end of the sixth transmembrane segment. Proc Natl Acad Sci USA 98:10055–10060.

Johnson LA, Furman CA, Zhang M, Guptaroy B, Gnegy ME. 2005. Rapid delivery of the dopamine transporter to the plasmalemmal membrane upon amphetamine stimulation. Neuropharmacology 49:750–758.

Jones SR, Gainetdinov RR, Wightman RM, Caron MG. 1998. Mechanisms of amphetamine action revealed in mice lacking the dopamine transporter. J Neurosci 18:1979–1986.
Jones SR, Joseph JD, Barak LS, Caron MG, Wightman RM. 1999. Dopamine neuronal transport kinetics and effects of amphetamine. J Neurochem 73:2406–2414.
Kahlig KM, Javitch JA, Galli A. 2004. Amphetamine regulation of dopamine transport—Combined measurements of transporter currents and transporter imaging support the endocytosis of an active carrier. J Biol Chem 279:8966–8975.
Kahlig KM, Binda F, Khoshbouei H, Blakely RD, McMahon DG, Javitch JA, Galli A. 2005. Amphetamine induces dopamine efflux through a dopamine transporter channel. Proc Nat Acad Sci USA 102:3495–3500.
Kahlig KM, Lute BJ, Wei Y, Loland CJ, Gether U, Javitch JA, Galli A. 2006. Regulation of dopamine transporter trafficking by intracellular amphetamine. Mol Pharmcol 70:542–548.
Kantor L, Gnegy ME. 1998. Protein kinase C inhibitors block amphetamine-mediated dopamine release in rat striatal slices. J Pharmacol Exp Ther 284:592–598.
Kantor L, Hewlett GHK, Park YH, Richardson-Burns SM, Mellon MJ, Gnegy ME. 2001. Protein kinase C and intracellular calcium are required for amphetamine-mediated dopamine release via the norepinephrine transporter in undifferentiated PC12 Cells. J Pharmacol Exp Ther 97:1016–1024.
Kantor L, Park YH, Wang KK, Gnegy ME. 2002. Enhanced amphetamine-mediated dopamine release develops in PC12 cells after repeated amphetamine treatment. Euro J Pharmacol 451:27–35.
Khoshbouei H, Wang H, Lechleiter JD, Javitch JA, Galli A. 2003. Amphetamine-induced dopamine efflux—A voltage-sensitive and intracellular Na^+-dependent mechanism. J Biol Chem 278:12070–12077.
Khoshbouei H, Sen N, Guptaroy B, Johnson L, Lund D, Gnegy ME, Galli A, Javitch JA. 2004. N-Terminal phosphorylation of the dopamine transporter is required for amphetamine-induced efflux. PLoS Biol 2:387–393.
Kuczenski R, Melega WP, Cho AK, Segal DS. 1997. Extracellular dopamine and amphetamine after systemic amphetamine administration: Comparison to the behavioral response. J Pharm Exp Ther 282:591–596.
Liang NY, Rutledge CO. 1982. Evidence for carrier-mediated efflux of dopamine from corpus striatum. Biochem Pharmacol 31:2479–2484.
Loder MK, Melikian HE. 2003. The dopamine transporter constitutively internalizes and recycles in a protein kinase C-regulated manner in stably transfected PC12 cell lines. J Biol Chem 278: 22168–22174.
Mack F, Bonisch H. 1979. Dissociation constants and lipophilicity of catecholamines and related compounds. Naunyn Schmiedebergs Arch Pharmacol 310:1–9.
Mason JN, Farmer H, Tomlinson ID, Schwartz JW, Savchenko V, DeFelice LJ, Rosenthal SJ, Blakely RD. 2005. Novel fluorescence-based approaches for the study of biogenic amine transporter localization, activity and regulation. J Neurosci Methods 143:3–25.
Melikian HE. 2004. Neurotransmitter transporter trafficking: Endocytosis, recycling and regulation. Pharmacol Therap 104:17–27.
Park YH, Kantor L, Guptaroy B, Zhang M, Wang KKW, Gnegy ME. 2003. Repeated amphetamine treatment induces neurite outgrowth and enhanced amphetamine-stimulated dopamine release in rat pheochromocytoma cells (PC12 cells) via a protein kinase C and mitogen activated protein kinase-dependent mechanism. J Neurochem 87:1546–1557.
Pifl C, Singer EA. 1999. Ion dependence of carrier-mediated release in dopamine or norepinephrine transporter-transfected cells questions the hypothesis of facilitated exchange diffusion. Mol Pharmacol 56:1047–1054.
Pifl C, Drobny H, Reither H, Hornykiewicz O, Singer EA. 1995. Mechanism of the dopamine-releasing actions of amphetamine and cocaine: Plasmalemmal dopamine transporter versus vesicular monoamine transporter. Mol Pharmacol 47:368–373.
Pristupa ZB, McConkey F, Liu F, Man HY, Lee FJ, Wang YT, Niznik HB. 1998. Protein kinase-mediated bidirectional trafficking and functional regulation of the human dopamine transporter. Synapse 30:79–87.
Romanenko VG, Gabera R, Miller KM, Njus D. 1998. Determination of transport parameters of permeant substrates of the vesicular amine transporter. Anal Biochem 257:127–133.
Rudnick G, Clark J. 1993. From synapse to vesicle: The reuptake and storage of biogenic amine neurotransmitters. Biochim Biophys Acta 1144:249–263.
Saunders C, Ferrer JV, Shi L, Chen J, Merrill G, Lamb ME, Leeb-Lundberg LMF, Carvelli L, Javitch JA, Galli A. 2000. Amphetamine-induced loss of human dopamine transporter activity: An internalization-dependent and cocaine-sensitive mechanism. Proc Natl Acad Sci USA 97:6850–6855.
Schenk JO. 2002. The functioning neuronal transporter for dopamine: Kinetic mechanisms and effects of amphetamines, cocaine and methylphenidate. Prog Drug Res 59:111–131.
Seiden LS, Sabol KE, Ricaurte GA. 1993. Amphetamine: Effects on catecholamine systems and behavior. Annu Rev Pharmacol Toxicol 32:639–677.
Sitte HH, Huck S, Reither H, Boehm S, Singer EA, Pifl C. 1998. Carrier-mediate release, transport rates and charge transfer induced by amphetamine, tyramine and dopamine in mammalian cells transfected with the human dopamine transporter. J Neurochem 71:1289–1297.
Sonders MS, Zhu SJ, Zahniser NR, Kavanaugh MP, Amara SG. 1997. Multiple ionic conductances of the human dopamine transporter: The actions of dopamine and psychostimulants. J Neurosci 17:960–974.
Stein WD. 1986. Transport and diffusion across cell membranes. Orlando: Academic Press.
Sulzer D, Maidment NT, Rayport S. 1993. Amphetamine and other weak bases act to promote reverse transport of dopamine in ventral midbrain neurons. J Neurochem 60:527–535.
Sulzer D, Sonders MS, Poulsen NW, Galli A. 2005. Mechanisms of neurotransmitter release by amphetamines: A review. Prog Neurobiol 75:406–433.
Troyer KP, Wightman R. 2002. Dopamine transport into a single cell in a picoliter vial. Anal Chem 74:5370–5375.
Wayment HK, Meiergerd SM, Schenk JO. 1998. Relationships between the catechol substrate binding site and amphetamine, cocaine and mazindol binding sites in a kinetic model of the striatal transporter of dopamine in vitro. J Neurochem 70:1941–1949.
Wilhelm CJ, Johnson RA, Eshleman AJ, Janowsky A. 2006. Hydrogen ion concentration differentiates effects of methamphetamine and dopamine on transporter-mediated efflux. J Neurochem 96:1149–1159.
Yamashita A, Singh SK, Kawate T, Jin Y, Gouaux E. 2005. Crystal structure of a bacterial homologue of Na^+/Cl^--dependent neurotransmitter transporters. Nature 437:215–223.
Zaczek R, Culp S, De Souza EB. 1991. Interactions of [3H] amphetamine with rat brain synaptosomes. II. Active transport. J Pharmacol Exp Ther 257:830–835.
Zahniser NR, Doolen S. 2001. Chronic and acute regulation of Na^+/Cl^- dependent neurotransmitter transporters: Drugs, substrates, presynaptic receptors and signaling systems. Pharmacol Ther 92: 21–55.
Zhang L, Coffey LL, Reith MEA. 1997. Regulation of the functional activity of the human dopamine transporter by protein kinase C. Biochem Pharmacol 53:677–688.

APPENDIX
AMPH-induced DA release kinetic model

The derivation of the ordinary differential equations describing the change in extracellular concentration of DA and AMPH with time is explained in this section. It is based on the transporter theory developed by Stein (1986).

For a simple uptake or release of a substrate (e.g., DA) through a membrane-bound transporter (e.g., DAT), the kinetic model is illustrated as below:

$$DA_i + DAT \underset{k_{-1}}{\overset{k_1}{\rightleftharpoons}} DA - DAT_i \underset{k_{-f}}{\overset{k_f}{\rightleftharpoons}} DA - DAT_0 \underset{k_{-2}}{\overset{k_2}{\rightleftharpoons}} DA_0 + DAT \qquad (A1)$$

where DA on the intracellular side (denoted by the subscript "i") binds reversibly to the inward-facing conformation of DAT existing in a dynamic equilibrium with the outward-facing conformation. DA then dissociates reversibly from the outward-facing transporter. The sequence will reverse for the uptake of DA from the outside the cell. By writing out the rate equations based on law of mass action, the rate of release of DA from inside to outside for zero-trans conditions can be given as

$$\frac{d[DA_o]}{dt}=\frac{k_2[DAT_t][DA_i]}{\left\{\left(\frac{k_2}{k_f}\right)\left(\frac{k_{-1}}{k_1}\right)+\left(\frac{k_{-1}}{k_1}\right)\left(\frac{k_{-f}}{k_f}\right)+\left(\frac{k_2}{k_1}\right)\right\}+[DA_i]}. \quad \text{(A1)}$$

This can be written in typical Michaelis–Menton form as $d[DA_o]/dt=(V_{max}[DA_i])/(K_m+[DA_i])$ where $V_{max}=k_2[DAT_t]$ and $K_m=((k_2/k_f)(k_{-1}/k_1))+((k_{-1}/k_1)\times(k_{-f}/k_f))+(k_2/k_1)$

For simultaneous transport of two substrates through the same transporter, we follow the scheme of Stein (1986). The kinetic scheme for the simultaneous transport of AMPH and DA through DAT (4-state model) is illustrated in Figure 1b.

For the scheme in Figure 1b, we have

$$\frac{[DAT_o]}{[DAT_t]}=\frac{F_1[DA_i]h_1B_2+h_1B_2k_1+B_1B_2k_1+g_2b_1k_1+f_1[AMPH_i]g_1b_2+g_1b_2k_1+b_2b_1k_1+b_1g_2k_1}{\Sigma} \quad \text{(A2a)}$$

$$\frac{[DAT_i]}{[DAT_t]}=\frac{F_2[DA_o]h_2B_1+h_1B_2k_2+B_1B_2k_2+h_2B_1k_2+f_2[AMPH_o]g_2b_1+g_1b_2k_2+b_2b_1k_2+b_1g_2k_2}{\Sigma} \quad \text{(A2b)}$$

$$\frac{[DAT_i-DA]}{[DAT_t]}=\frac{F_1[DA_i]k_2B_2+h_2F_2[DA_i]k_1+h_2F_1[DA_i]k_2+h_2F_1F_2[DA_o][DA_i]}{\Sigma} \quad \text{(A2c)}$$

$$\frac{[DAT_o-DA]}{[DAT_t]}=\frac{F_2[DA_o]k_1B_1+k_2F_1[DA_i]h_1+h_1F_2[DA_o]k_1+h_1F_1F_2[DA_o][DA_i]}{\Sigma} \quad \text{(A2d)}$$

$$\frac{[DAT_o-AMPH]}{[DAT_t]}=\frac{f_2[AMPH_o]k_1b_1+k_2f_1[AMPH_i]g_1+h_1f_2[AMPH_o]k_1+g_1f_1f_2[AMPH_o][AMPH_t]}{\Sigma} \quad \text{(A2e)}$$

$$\frac{[DAT_i-AMPH]}{[DAT_t]}=\frac{f_1[AMPH_i]k_2b_2+k_1f_2[AMPH_o]g_2+g_2f_1[AMPH_i]k_2+g_2f_1f_2[AMPH_o][AMPH_i]}{\Sigma} \quad \text{(A2f)}$$

where, Σ = sum of numerators of the right hand side of all the six Eqs. A2a–A2f.

Following the method of analysis suggested by Britton (1977), the unidirectional flux from inside to outside is given by

$$-\frac{d[DA_i]}{dt}=\frac{d[DA_o]}{dt}=F_1[DA_i]\left(\frac{h_1}{B_1+h_1}\right)\times\left(\frac{B_2}{B_2+\left(\frac{h_2B_1}{B_1+h_1}\right)}\right)[DAT_i]. \quad \text{(A3)}$$

Upon substituting the expression for $[DAT_i]$, we get

$$-\frac{d[DA_i]}{dt}=\frac{d[DA_o]}{dt}=[DA_i]\frac{F_1h_1B_2}{B_1B_2+B_2h_1+h_2B_1}[DAT_t]\times\left\{\frac{F_2[DA_o]h_2B_1+h_1B_2k_2+B_1B_2k_2+h_2B_1k_2+f_2[AMPH_o]g_2b_1+g_1b_2k_2+b_2b_1k_2+b_1g_2k_2}{\Sigma}\right\}. \quad \text{(A4)}$$

For zero trans conditions, the initial concentration of DA_o will be zero and even during the course of release, the value of DA_o is very low. Also, there is no intracellular AMPH initially. Considering all these, Eq. A4 simplifies to give the overall DA release rate as

$$-\frac{d[DA_i]}{dt}=\frac{d[DA_o]}{dt}=\frac{V_1'[DA_i]+V_2'[DA_i][AMPH_o]}{K_1'+a'[AMPH_o]+b[DA_i]} \quad \text{(A5)}$$

where

$$V_1'=(h_1B_2k_2+B_1B_2k_2+h_2B_1k_2+g_1b_2k_2+b_2b_1k_2+b_1g_2k_2)\frac{F_1h_1B_2}{B_1B_2+B_2h_1+h_2B_1}[DAT_t] \quad \text{(A6)}$$

$$V_2'=(f_2g_2b_1)\frac{F_1h_1B_2}{B_1B_2+B_2h_1+h_2B_1}[DAT_t] \quad \text{(A7)}$$

$$K_1' = h_1B_2k_1 + B_1B_2k_1 + g_2b_1k_1 + g_1b_2k_1 + b_2b_1k_1 + b_1g_2k_1 + h_1B_2k_2 + B_1B_2k_2 + h_2B_1k_2 + g_1b_2k_2 + b_2b_1k_2 + b_1g_2k_2 \quad \text{(A8)}$$

$$a' = f_2(g_2b_1 + k_1b_1 + h_1k_1 + k_1g_2) \quad \text{(A9)}$$

$$b = F_1(h_1B_2 + k_2B_2 + h_2k_2 + k_2h_1) + h_2F_2k_1. \quad \text{(A10)}$$

Equation A5 can be written as the sum of two terms, thereby uncoupling the basal DA release and the AMPH-induced DA release as follows:

$$-\frac{d[DA_i]}{dt} = \frac{d[DA_o]}{dt} = \frac{\left(\frac{V_1'}{b}\right)[DA_i]}{\left(\frac{K_1'}{b}\right) + [DA_i]} + \frac{\left(\frac{V_2'}{b}\right)[DA_i][AMPH_o]}{\left(\frac{K_1'}{b}\right) + \left(\frac{a'}{b}\right)[AMPH_o] + [DA_i]} \quad \text{(A11)}$$

Rewriting the earlier equation,

$$-\frac{d[DA_i]}{dt} = \frac{d[DA_o]}{dt} = \frac{V_1[DA_i]}{K_1 + [DA_i]} + \frac{V_2[DA_i][AMPH_o]}{K_1 + a[AMPH_o] + [DA_i]}. \quad \text{(A11a)}$$

Normalizing the concentration of membrane-bound DAT at any point of time to that at time $t = 0$ in the earlier equation, we obtain

$$-\frac{d[DA_i]}{dt} = \frac{d[DA_o]}{dt} = \frac{p_1\,\tilde{n}(t)[DA_i]}{K_1 + [DA_i]} + \frac{p_2\,\tilde{n}(t)[DA_i][AMPH_o]}{K_1 + a[AMPH_o] + [DA_i]} \quad \text{(A12)}$$

where

$$p_1 = \frac{V_1'}{b} = \frac{(h_1B_2k_2 + B_1B_2k_2 + h_2B_1k_2 + g_1b_2k_2 + b_2b_1k_2 + b_1g_2k_2)\frac{F_1h_1B_2}{B_1B_2 + B_2h_1 + h_2B_1}[DAT_t]_{t=0}}{F_1(h_1B_2 + k_2B_2 + h_2k_2 + k_2h_1) + h_2F_2k_1} \quad \text{(A13)}$$

$$p_2 = \frac{V_2'}{b} = \frac{(f_2g_2b_1)\frac{F_1h_1B_2}{B_1B_2 + B_2h_1 + h_2B_1}[DAT_t]_{t=0}}{F_1(h_1B_2 + k_2B_2 + h_2k_2 + k_2h_1) + h_2F_2k_1} \quad \text{(A14)}$$

$$K_1 = \frac{K_1'}{b} = \frac{h_1B_2k_1 + B_1B_2k_1 + g_2b_1k_1 + g_1b_2k_1 + b_2b_1k_1 + b_1g_2k_1 + h_1B_2k_2 + B_1B_2k_2 + h_2B_1k_2 + g_1b_2k_2 + b_2b_1k_2 + b_1g_2k_2}{F_1(h_1B_2 + k_2B_2 + h_2k_2 + k_2h_1) + h_2F_2k_1} \quad \text{(A15)}$$

$$a = \frac{f_2(g_2b_1 + k_1b_1 + h_1k_1 + k_1g_2)}{F_1(h_1B_2 + k_2B_2 + h_2k_2 + k_2h_1) + h_2F_2k_1} \quad \text{(A16)}$$

$$\tilde{n}(t) = \frac{[DAT_t]}{[DAT_t]_{t=0}} \quad \text{(A17)}$$

Intracellular concentration of AMPH

In our AMPH perfusion experiments, the extracellular AMPH concentration was maintained constant. The intracellular concentration of AMPH will eventually reach a constant steady state value after some finite time of DAT-mediated transport. A simple expression for this steady state concentration of intracellular AMPH can be deduced as follows:

Rate of increase of intracellular AMPH following transport from outside is given by

$$\frac{d[AMPH_i]}{dt} = \frac{V_4[AMPH_o]}{K_4 + [AMPH_o]} - \frac{V_5[AMPH_i]}{K_5 + [AMPH_i]}. \quad \text{(A18)}$$

Since $[AMPH_i]$ is significantly smaller than K_5, this can be simplified to

$$\frac{d[AMPH_i]}{dt} = \frac{V_4[AMPH_o^*]}{K_4 + [AMPH_o^*]} - \frac{V_5}{K_5}[AMPH_i] \qquad \text{(A19)}$$

where $[AMPH_o^*]$ is the constant outside concentration of extracellular AMPH.

Equation A18, on simplification yields

$$[AMPH_i] = \frac{V_4[AMPH_o^*]}{K_4 + [AMPH_o^*]}\frac{1}{\beta}\left(1 - e^{-\beta t}\right) \qquad \text{(A20)}$$

where $\beta = \frac{V_5}{K_5}$.